

Figure 1: Satellite imagery of study area.

Vista Alegre is a small island on the north coast of the Yucatan Peninsula, at the southern edge of Holbox Lagoon. Architectural features such as a pyramid and defensive wall mark it as an important maritime trading settlement for the northern Maya lowlands, with evidence of occupation from c. 8th century BCE-16th century CE. The island is bounded by shallow bays to the east and west, which are thought to have been maintained in antiquity to harbor large dugout canoes that facilitated circum-peninsular trade.

In 2016, archeologists opened a series of 1m x 1m test excavations in an east-west transect across the island, reaching depths of up to 3.97m before encountering bedrock (Glover and Rissolo 2017). This depth of sediment is considered anomalous for the region, which is characterized by poorly developed soil profiles overlaying a recently emerged carbonate platform. The island's localized high volume of sediment deposition is thought to be the result, in part, of anthropogenic processes such as dredging, filling, and levelling.

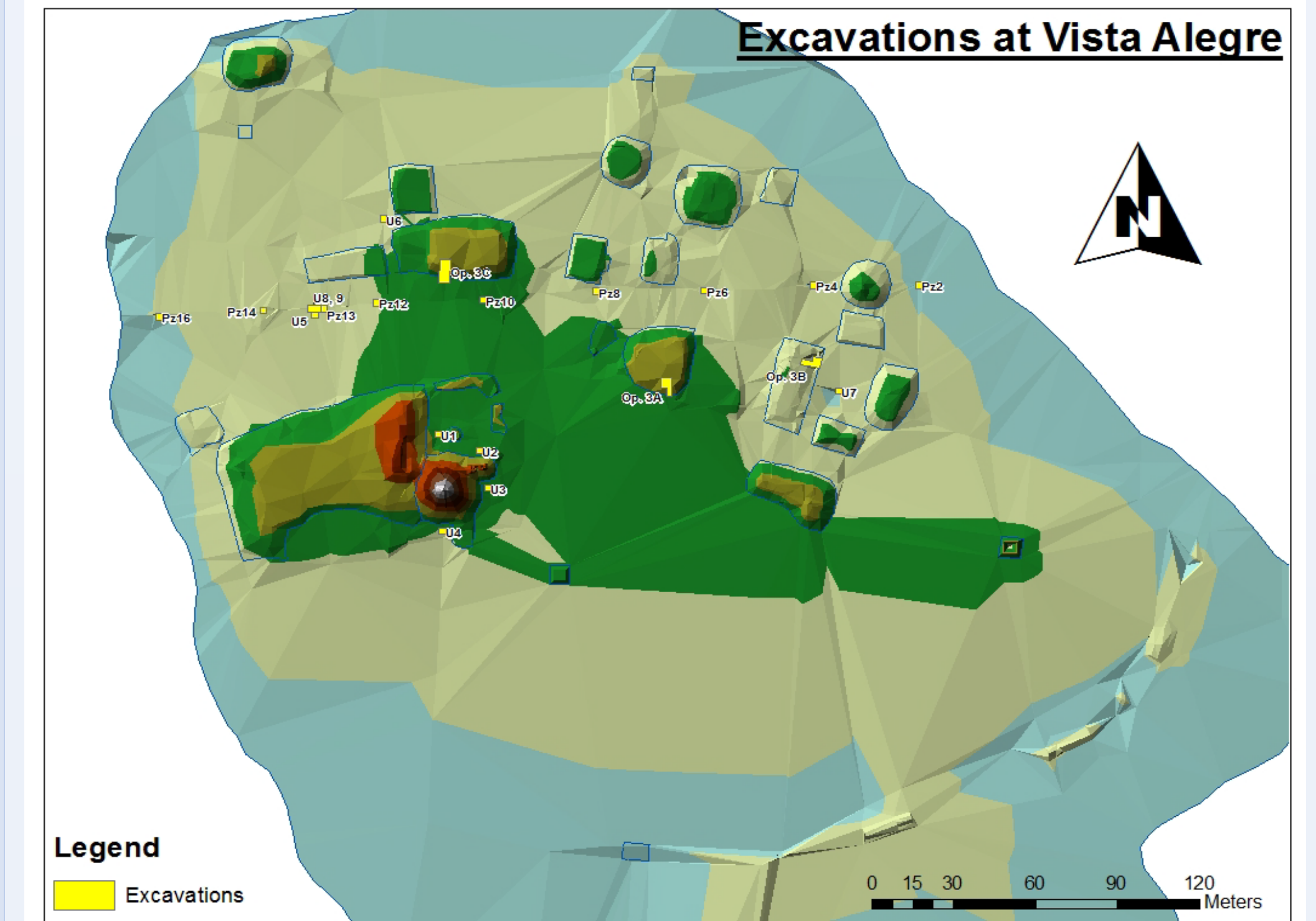


Figure 2: Excavations at Vista Alegre. This study analyzed samples from Pz16, Pz14, U8, Pz13, Pz12, Pz8, Pz6, Pz4, and Pz2.

MATERIALS & METHODS

A total of 67 sediment samples were collected during the 2016 excavations, based on:

- Visually determined sedimentary strata (33)
- Archaeological level (7)
- Ash lenses or other cultural features (22)
- Stratigraphic anomalies (5)

Samples were sealed in Whirl-Pak baggies for future analysis, with the goal of investigating the island's formation processes.

In May 2021, FP-XRF analysis was performed using a Bruker Tracer 5i unit. Each sample was analyzed using both the 15kV and 40kV mud rock settings. Three measurements were taken for each sample at each setting, with a 120 second duration. The instrument was configured for hands-free remote operation to ensure measurement consistency.




Figure 3: Instrument configured for remote operation. Inset shows sample placement on stage.

ANALYSIS

After collection, data were separated out by excavation and converted from percentage to ppm. To select analytes for FP-XRF geochemistry, correlation matrices were constructed for each excavation using the VassarStats.net Matrix of Intercorrelation function (see Table 1). Values of $|r| = 0.95$ or greater were considered as statistically significant correlations.

These matrices were then compiled into an overview (see Table 2) for visual reference. The following analytes were selected for use:

- Si (15kV)
- Ca (15kV)
- Ti (15kV)
- Mn (15kV)
- Fe (15kV)
- Ti (40kV)
- Fe (40kV)
- Co (40kV)

ANALYSIS (cont'd)

Each sample was assigned a depth value. Actual depth was used if available, otherwise the median value of the recorded stratum or level was estimated based on excavation profile sketches. Each analyte was then plotted against the profile sketch of each excavation, to examine changes in concentration with depth.

Table 1: Example correlation matrix (Pozo 14).

	Si	Ca	Ti	Mn	Fe	Co	Al	Si	Ca	Ti	Mn	Fe	Co	Al	Si	Ca	Ti	Mn	Fe	Co	Al
Si	1.00	0.95	0.92	0.88	0.85	0.82	0.79	0.76	0.73	0.70	0.67	0.64	0.61	0.58	0.55	0.52	0.49	0.46	0.43	0.40	0.37
Ca	0.95	1.00	0.93	0.90	0.87	0.84	0.81	0.78	0.75	0.72	0.69	0.66	0.63	0.60	0.57	0.54	0.51	0.48	0.45	0.42	0.39
Ti	0.92	0.93	1.00	0.95	0.92	0.89	0.86	0.83	0.80	0.77	0.74	0.71	0.68	0.65	0.62	0.59	0.56	0.53	0.50	0.47	0.44
Mn	0.88	0.90	0.95	1.00	0.95	0.92	0.89	0.86	0.83	0.80	0.77	0.74	0.71	0.68	0.65	0.62	0.59	0.56	0.53	0.50	0.47
Fe	0.85	0.87	0.92	0.95	1.00	0.95	0.92	0.89	0.86	0.83	0.80	0.77	0.74	0.71	0.68	0.65	0.62	0.59	0.56	0.53	0.50
Co	0.82	0.84	0.89	0.92	0.95	1.00	0.95	0.92	0.89	0.86	0.83	0.80	0.77	0.74	0.71	0.68	0.65	0.62	0.59	0.56	0.53
Al	0.79	0.81	0.86	0.89	0.92	0.95	1.00	0.95	0.92	0.89	0.86	0.83	0.80	0.77	0.74	0.71	0.68	0.65	0.62	0.59	0.56
Si	0.76	0.78	0.83	0.86	0.89	0.92	0.95	1.00	0.95	0.92	0.89	0.86	0.83	0.80	0.77	0.74	0.71	0.68	0.65	0.62	0.59
Ca	0.73	0.75	0.80	0.83	0.86	0.89	0.92	0.95	1.00	0.95	0.92	0.89	0.86	0.83	0.80	0.77	0.74	0.71	0.68	0.65	0.62
Ti	0.70	0.72	0.77	0.80	0.83	0.86	0.89	0.92	0.95	1.00	0.95	0.92	0.89	0.86	0.83	0.80	0.77	0.74	0.71	0.68	0.65
Mn	0.67	0.69	0.74	0.77	0.80	0.83	0.86	0.89	0.92	0.95	1.00	0.95	0.92	0.89	0.86	0.83	0.80	0.77	0.74	0.71	0.68
Fe	0.64	0.66	0.71	0.74	0.77	0.80	0.83	0.86	0.89	0.92	0.95	1.00	0.95	0.92	0.89	0.86	0.83	0.80	0.77	0.74	0.71
Co	0.61	0.63	0.68	0.71	0.74	0.77	0.80	0.83	0.86	0.89	0.92	0.95	1.00	0.95	0.92	0.89	0.86	0.83	0.80	0.77	0.74
Al	0.58	0.60	0.65	0.68	0.71	0.74	0.77	0.80	0.83	0.86	0.89	0.92	0.95	1.00	0.95	0.92	0.89	0.86	0.83	0.80	0.77

Table 2: Overview of elements which displayed correlations for each excavation.

	P16	P14	U8	P13	P12	P12A	P12B	P8	P8A	P4A	P2
Na15											
Mg15											
Al15											
Si15											
P15											
Si15											
K15											
Ca15											
Ti15											
V15											
Cr15											
Mn15											
Fe15											
Ba15											
K40											
Ca40											
Ti40											
V40											
Cr40											
Mn40											
Fe40											
Co40											
Ni40											
Cu40											
Zn40											
Ga40											
As40											
Se40											
Rb40											
Sr40											
V40											
Zn40											
Nb40											
Mo40											
Ba40											
Pb40											
Th40											
U40											

DISCUSSION

- Negative correlation between Ca and Si likely indicates carbonate vs. siliciclastic sediments, respectively.
- Intercorrelation observed between Fe/Mn/Ti (15kV) may indicate presence of Ti-bearing minerals such as Ilmenite or Rutile. (Meyer, 2013)
- Moving forward, FP-XRF results will be compared against the lithology of the samples to determine trends in elemental abundance and mineralogy. An attempt will also be made to evaluate the ratios of elements that may indicate anthropogenic influences.

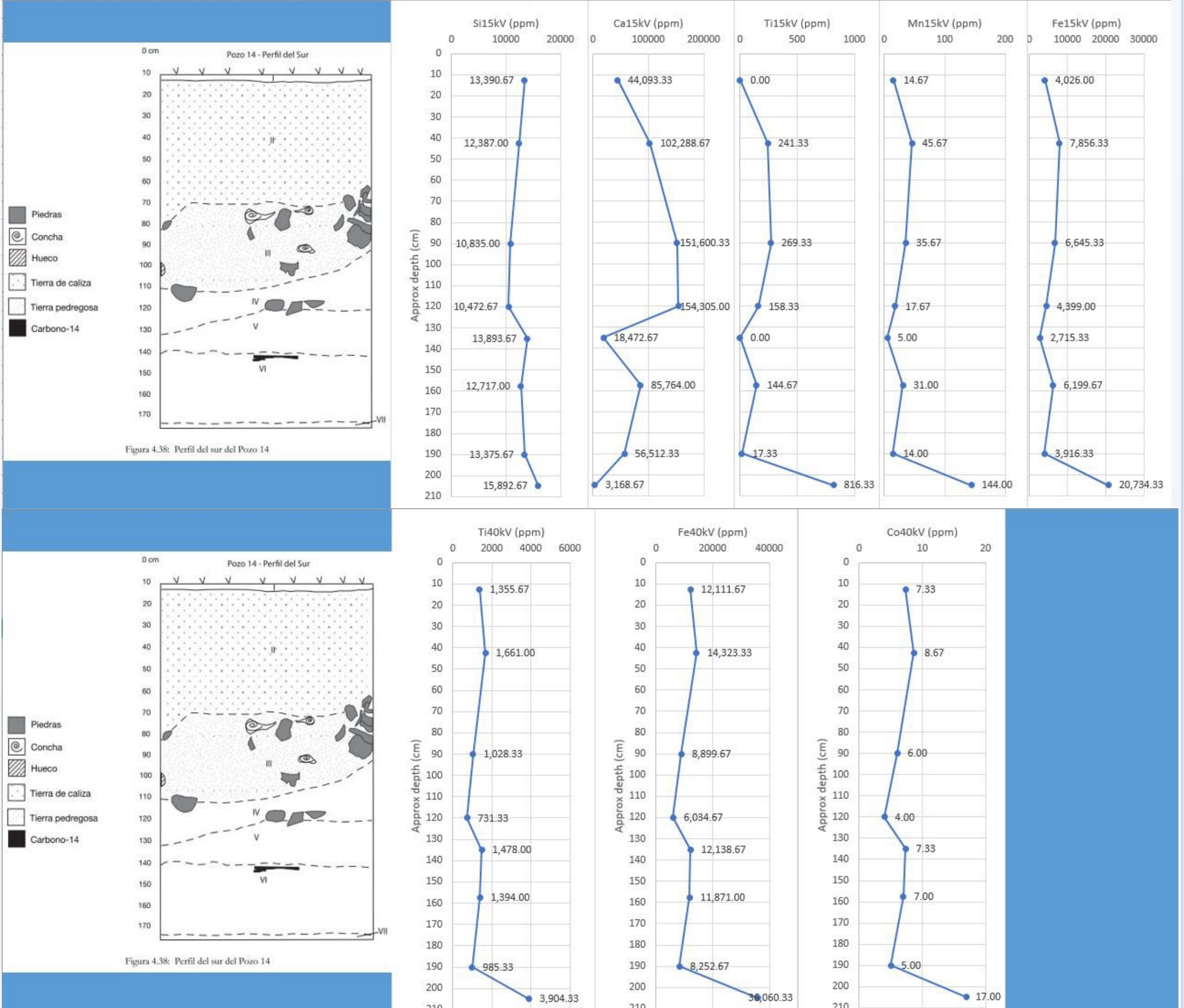


Figure 4: Example depth plots for 15kV (top) and 40kV (bottom) analytes (Pozo 14). Sketch from Glover and Rissolo 2017.

ACKNOWLEDGEMENTS

The authors wish to thank:

- Dr. Nicola Sharratt², for her loan of the Bruker Tracer 5i and advice on setup.
- Dr. Lawrence M. Kiage¹, for his assistance with importation of the samples.
- GSA Southeastern Section, for their support via travel grant.
- Sigma Gamma Epsilon (Epsilon Rho chapter) and GSU Geosciences Graduate Student Alliance, for additional support.

REFERENCES

Glover, Jeffrey B. and Dominique Rissolo (editors)
2017 *El Proyecto Costa Escondida: Una Investigación Arqueológica y Paleoambiental de dos Puertos Maya, Vista Alegre y Conil, y la Costa Norte de Quintana Roo, México. Temporada de campo Enero - Junio 2016. Informe Técnico Anual* preparado para el Consejo de Arqueología del Instituto Nacional de Antropología e Historia, México, D.F.

Meyer, Brian K.
2013 *Shoreline Dynamics and Environmental Change Under the Modern Marine Transgression: St. Catherines Island, Georgia. PhD Dissertation*, Department of Geosciences, Georgia State University, Atlanta. https://scholarworks.gsu.edu/geosciences_diss/5